Research

Genomic-scale measurement of mRNA turnover and the mechanisms of action of the anti-cancer drug flavopiridol

Lloyd T Lam*, Oxana K Pickeral*, Amy C Peng[†], Andreas Rosenwald*, Elaine M Hurt*, Jena M Giltnane*, Lauren M Averett*, Hong Zhao*, R Eric Davis*, Mohan Sathyamoorthy*, Larry M Wahl[‡], Eric D Harris[§], Judy A Mikovits[§], Anne P Monks[§], Melinda G Hollingshead[§], Edward A Sausville[§] and Louis M Staudt*

Addresses: *Metabolism Branch, Center for Cancer Research, National Cancer Institute, National Institutes of Health, Bethesda, MD 20892, USA. [†]The EMMES Corporation, 401 N Washington Street, Suite 700, Rockville, MD 20850, USA. [‡]National Institute for Dental and Craniofacial Research, National Institutes of Health, Bethesda, MD 20892, USA. [§]Developmental Therapeutics Program, DTP Clinical Trials Unit, Division of Cancer Treatment and Diagnosis, National Cancer Institute, Bethesda, MD 20892, USA.

Correspondence: Louis M Staudt. E-mail: lstaudt@box-l.nih.gov

Abstract

Background: Flavopiridol, a flavonoid currently in cancer clinical trials, inhibits cyclin-dependent kinases (CDKs) by competitively blocking their ATP-binding pocket. However, the mechanism of action of flavopiridol as an anti-cancer agent has not been fully elucidated.

Results: Using DNA microarrays, we found that flavopiridol inhibited gene expression broadly, in contrast to two other CDK inhibitors, roscovitine and 9-nitropaullone. The gene expression profile of flavopiridol closely resembled the profiles of two transcription inhibitors, actinomycin D and 5,6-dichloro-1-β-D-ribofuranosyl-benzimidazole (DRB), suggesting that flavopiridol inhibits transcription globally. We were therefore able to use flavopiridol to measure mRNA turnover rates comprehensively and we found that different functional classes of genes had distinct distributions of mRNA turnover rates. In particular, genes encoding apoptosis regulators frequently had very short half-lives, as did several genes encoding key cell-cycle regulators. Strikingly, genes that were transcriptionally inducible were disproportionately represented in the class of genes with rapid mRNA turnover.

Conclusions: The present genomic-scale measurement of mRNA turnover uncovered a regulatory logic that links gene function with mRNA half-life. The observation that transcriptionally inducible genes often have short mRNA half-lives demonstrates that cells have a coordinated strategy to rapidly modulate the mRNA levels of these genes. In addition, the present results suggest that flavopiridol may be more effective against types of cancer that are highly dependent on genes with unstable mRNAs.

Background

DNA microarrays have proven very useful in establishing molecular definitions of human cancer subtypes [1-3]. In some cases, cancers that were assigned to a single diagnostic category by conventional morphological diagnostic methods have been found to have different gene expression profiles

and belong to distinct molecular subtypes. In particular, diffuse large B-cell lymphoma (DLBCL) was shown to consist of at least two molecular subtypes that differed in the expression of over several hundred genes [1]. Furthermore, patients with these two DLBCL subtypes had strikingly different long-term outcomes following conventional multi-agent chemotherapy. Patients with germinal center B-like DLBCL had a favorable prognosis, with an apparent cure rate of 75%. On the other hand, patients with activated B-like DLBCL had a poor prognosis, with less than a quarter of these patients alive five years following therapy. Therefore, for patients with activated B-like DLBCL, alternative therapeutic agents must be identified.

For this reason, we have begun a survey of novel cancer agents in order to identify drugs with significant activity against activated B-like DLBCL. One drug identified in this screen, flavopiridol, was found to be significantly cytotoxic for cell lines derived from activated B-like DLBCL. Flavopiridol is a member of the growing family of cyclin-dependent kinase (CDK) inhibitors that have varying activities against the multiple CDK family members (CDK1, CDK2, CDK4, CDK6 and CDK7) by competitively blocking their ATP-binding pocket [4-8]. In addition to arresting cells *in vitro* at the G2-to-M and the G1-to-S transitions, flavopiridol decreases the rate of progression through S phase. Since flavopiridol is being evaluated in multiple cancer clinical trials [7,9], and has been shown to be highly active in inducing apoptosis in hematopoietic neoplasms [10], we were interested in whether flavopiridol might be effective against activated B-like DLBCL.

Although it is clear that flavopiridol inhibits CDKs, whether flavopiridol inhibits other cellular targets is not known. Recently, flavopiridol was found to inhibit the activity of a transcription elongation factor P-TEFb, a complex of cyclins with CDK9 [11]. P-TEFb phosphorylates the carboxy-terminal domain of the RNA polymerase II complex [12], facilitating transcription elongation. It was not known, however, whether P-TEFb regulates transcriptional elongation of all cellular genes or whether other factors promote transcriptional elongation on subsets of cellular genes.

Using DNA microarrays, we found that flavopiridol inhibited gene expression broadly in a manner highly related to other transcription inhibitors such as actinomycin D and 5,6-dichloro-1-β-D-ribofuranosyl-benzimidazole (DRB). We were therefore able to use flavopiridol to study the turnover rate of mRNA on a genomic-scale. mRNA turnover is regulated by a variety of cellular factors acting on *cis*-elements in mRNA molecules. For many labile mRNAs, adenylate uridylate-rich elements (AREs) are required for their rapid degradation. Three different classes of ARE have been defined [13]. A conserved motif present in two of these classes, AUUUA, plays an important role in transcript stability for many cytokines and early-response genes (ERGs)

[13]. However, there is now increasing evidence that other motifs may determine the stability of transcripts [14].

By measuring mRNA turnover rates comprehensively, we identified unexpected relationships between the function of a gene and its mRNA stability. In addition, we found that genes that were transcriptionally inducible were disproportionately represented in the class of genes with labile mRNAs, thus revealing a coordinated strategy to rapidly modulate the mRNA levels of these genes. This understanding of mRNA turnover on a genomic scale provides fresh insights into the effectiveness of flavopiridol as an anticancer agent.

Results and discussion

To investigate the effect of flavopiridol treatment on activated B-like DLBCL, we used cell line OCI-Ly3 as our model of activated B-like DLBCL as its gene-expression profile closely resembles the profiles of lymphoma biopsy samples from patients with this type of DLBCL [1]. OCI-Ly3 were treated for 3 hours with flavopiridol (1 μM) and gene expression changes were monitored using Lymphochip DNA microarrays [15]. In comparison to untreated OCI-Ly3 cells, flavopiridol treatment decreased expression of 284 out of 5,032 microarray elements (5.64%) by at least twofold (data not shown). Similarly, profound decreases in mRNA levels were observed following flavopiridol treatment of other lymphoma cell lines (data not shown). The magnitude of the flavopiridol effect on gene expression was related to the dose of the drug used (Figure 1a). We found that there was almost no effect on gene expression in cells treated with 60 nM flavopiridol for 1 and 3 hours whereas 300 nM flavopiridol induced broad changes in gene expression, and 1 mM flavopiridol was yet more potent in decreasing mRNA levels. Patients receiving infusions of flavopiridol achieve a biologically active concentration in plasma of 300 nM [16]. To relate these gene expression changes to the biological activity of flavopiridol, we assayed the viability of OCI-Ly3 cells treated with different doses of flavopiridol (Figure 1b). Flavopiridol at a concentration of 60 nM had no effect on viability even after 48 hours treatment. In contrast, 250 nM flavopiridol decreased the viability of OCI-Ly3 cells at 8 hours. Given the similar dose-response effects of flavopiridol on cytotoxicity and gene expression, it is likely that the global reduction in mRNA levels caused by flavopiridol is a major contributor to its cytotoxic action.

Flavopiridol is a member of the growing family of CDK inhibitors that have varying activities against the multiple CDK family members. As most of the CDK inhibitors bind to the ATP-binding pocket of the CDKs [17], and all CDKs have similar ATP-binding pockets, it was possible that other CDK inhibitors also inhibit transcription. We determined whether the inhibition of transcription is specific to flavopiridol by comparing gene expression profiles of flavopiridol-treated
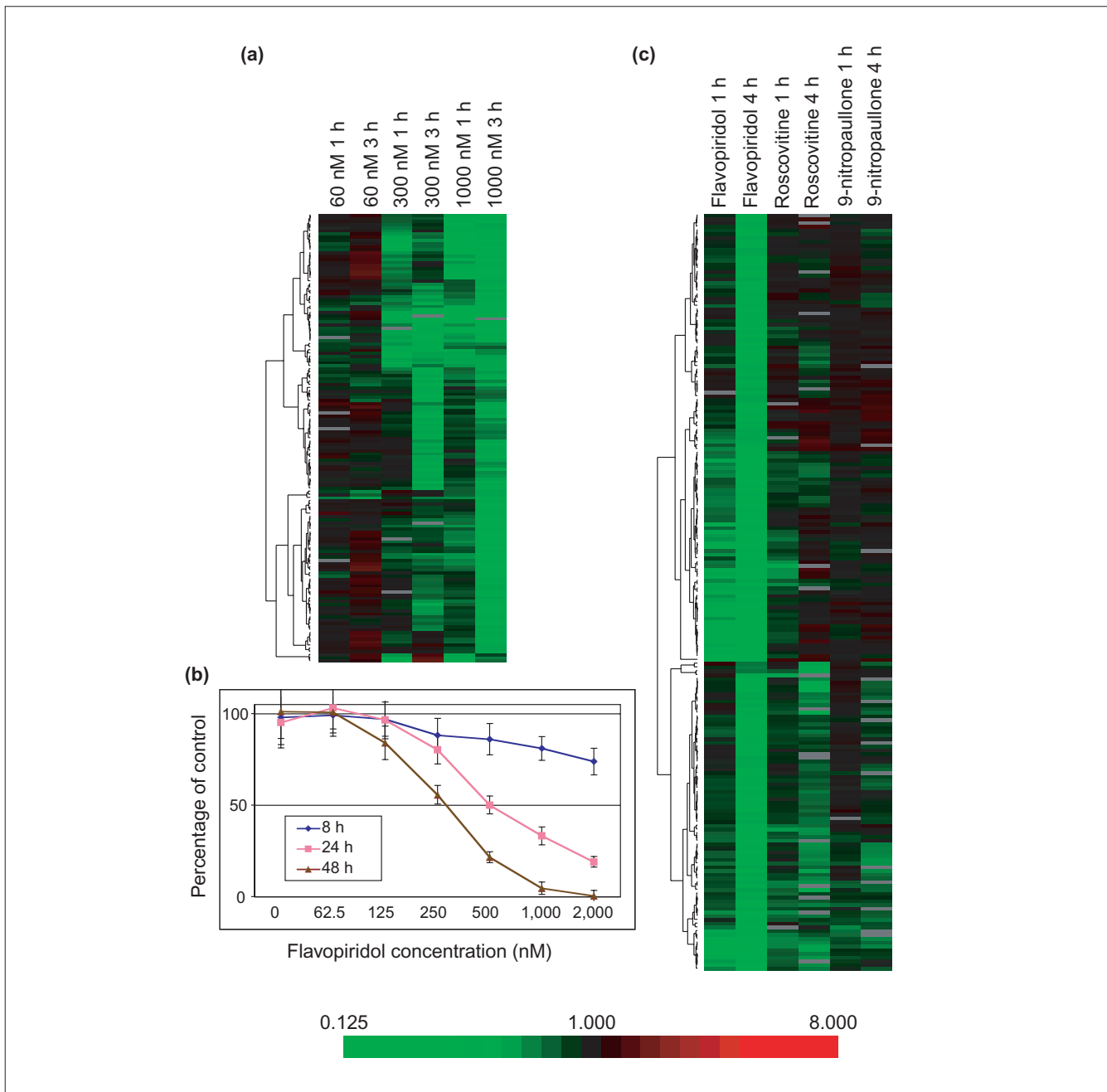
Figure 1
Gene expression patterns of lymphoma cell line OCI-Ly3 treated with flavopiridol. **(a)** Hierarchical clustering of OCI-Ly3 cells treated with 60 nM, 300 nM, or 1 μM flavopiridol for 1 or 3 h. Each column is a single experiment comparing two cDNA populations; treated sample was labeled red (Cy5) and untreated sample was labeled green (Cy3). Each row represents data from a single cDNA microarray spot. The red-to-green (Cy5/Cy3) ratio reflects hybridization to that spot, a measure of relative gene expression; intensity reflects the magnitude of the difference between the samples according to the ratio color scale. Red indicates Cy5/Cy3 ratios > 1, green indicates Cy5/Cy3 ratios < 1, black indicates no significant change in gene expression, and gray indicates the spot did not meet data selection criteria. These ratios were depicted according to the color scale shown at the bottom. **(b)** MTT assays. OCI-Ly3 cells were treated with increasing concentration of flavopiridol (0 to 2 μM) for 8, 24 or 48 h. MTT was added to the cells 2 h before harvesting. The plate was read at 570 nm. The result was shown as percentage of control versus flavopiridol concentration. **(c)** Hierarchical clustering of OCI-Ly3 cells treated with flavopiridol (1 μM), roscovitine (25 μM), or 9-nitropaullone (2.5 μM) for 1 or 4 h. These concentrations were chosen to give roughly equivalent (approximately 50%) cytotoxicity at 24 h without significant loss of cell viability at 8 h. The treated samples were labeled red (Cy5) and untreated samples were labeled green (Cy3). Only genes that were downregulated by more than threefold in one or more samples were extracted for clustering.

cells with those of cells treated with the CDK inhibitors roscovitine and 9-nitropaullone. Roscovitine is a purine derivative that inhibits CDK1, CDK2 and CDK5 and blocks cell-cycle progression both in late G1/early S and in M phase [18-21]. 9-nitropaullone, the most potent member of a novel class of the paullone CDK inhibitor family, inhibits CDK1/cyclin B at 10-fold lower concentrations than flavopiridol and roscovitine [22-24]. As shown in Figure 1c, the gene expression changes caused by roscovitine and 9-nitropaullone were different from those of flavopiridol, and only flavopiridol globally reduced mRNA levels.

To determine whether flavopiridol affects transcription globally, we compared the gene expression profile of flavopiridol treatment with the gene expression profiles induced in OCI-Ly3 cells by treatment with two well-studied transcriptional

inhibitors, actinomycin D and DRB. Actinomycin D inhibits transcription initiation broadly by intercalating into DNA whereas DRB inhibits the transcription elongation factor P-TEFb [12]. P-TEFb is a complex of cyclins with CDK9, and flavopiridol can also inhibit this kinase [11]. However, it was not known whether P-TEFb regulates transcriptional elongation of all cellular genes, nor was it known whether flavopiridol would inhibit the same set of genes as DRB. OCI-Ly3 cells were treated with each inhibitor, and the resultant changes in gene expression were found to be virtually indistinguishable (Figure 2a). For the majority of well-measured genes on the Lymphochip, the mRNA abundance decreased with first-order kinetics (Figure 3) and could therefore be used to measure mRNA turnover rates (see Materials and methods). Genes are grouped according to mRNA half-life in Figure 2a. The turnover rates of representative mRNAs were
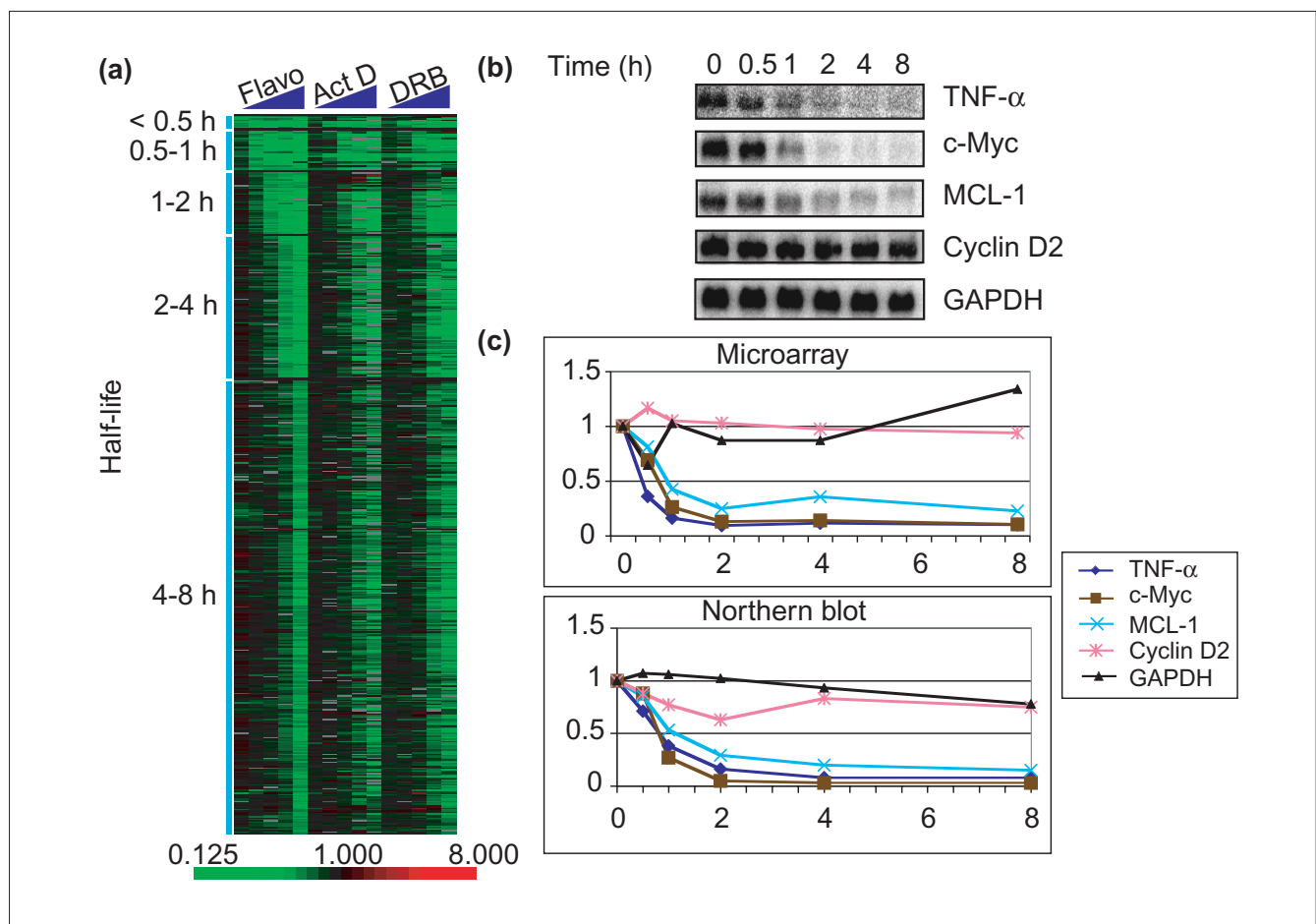
Figure 2
Similar gene expression patterns of OCI-Ly3 cells treated with flavopiridol, actinomycin D and DRB. **(a)** OCI-Ly3 cells were treated with flavopiridol (1 μM), actinomycin D (10 μg/ml), or DRB (100 μM) for 0.5, 1, 2, 4 and 8 h. These concentrations were chosen to give roughly equivalent (approximately 50%) cytotoxicity at 24 h without significant loss of cell viability at 8 h. The treated samples were labeled red (Cy5) and untreated samples were labeled green (Cy3). Genes were categorized according to their half-lives by the scheme as described in Materials and methods. **(b)** Northern blot analysis of selected genes. **(c)** Comparison of turnover rate of selected genes from microarray data and Northern blot analysis (percentage of control versus time).

verified by northern blot analysis in Figure 2b and quantitated in Figure 2c. These findings demonstrate that all three compounds behave as global inhibitors of transcription, and demonstrate that P-TEFb regulates the transcriptional elongation of most cellular genes. Further, the similar effects of flavopiridol and DRB argue that the predominant effect of flavopiridol on gene expression results from its ability to inhibit P-TEFb.

To investigate whether the mRNA degradation rates were first-order, we fitted a linear regression model for the three drugs for each gene (see Materials and methods). The adjusted R-squared statistic, which is a measure of correlation between the observed data values and the predicted values from the linear model, shows how well a first-order kinetics model would describe the mRNA degradation rates. Figure 3 shows a histogram of the adjusted R-squared statistics obtained from fitting a model for each of the 2,794 genes. The median adjusted R-squared was 0.86, and 79.7% of the genes had an adjusted R-squared statistic over 0.7, showing that most of the genes had first-order mRNA degradation rates.

Given the demonstration that flavopiridol is a global transcriptional inhibitor, we wished to understand the selective activity of flavopiridol against certain cancer types *in vivo*. Clearly, genes with short mRNA half-lives would be most rapidly and quantitatively inhibited by flavopiridol, and thus we wished to assign the genes with short half-lives in OCI-Ly3 cells to functional classes. First, we searched for genes involved in cellular proliferation that have unstable mRNAs, as decreased expression of these genes might provide a mechanism by which flavopiridol preferentially targets proliferating cancer cells. Microarray gene expression analysis
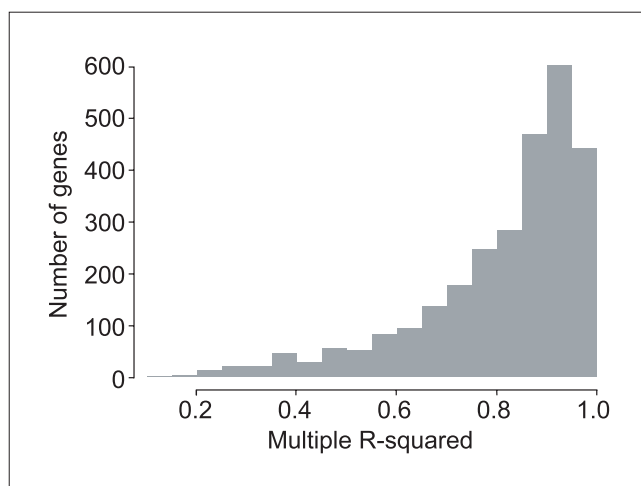

Figure 3
The majority of well-measured genes on the Lymphochip decreased in mRNA abundance with first-order kinetics after transcriptional inhibition. See text for details.

can readily identify a proliferation 'signature' consisting of hundreds of genes that vary in expression between proliferating and quiescent cells [1,25]. Genes can be assigned to the proliferation signature on the basis of high expression in diverse cell lines and low expression in chronic lymphocytic leukemia (CLL), a malignancy in which the leukemic cells are primarily in G0/G1 phase of the cell cycle [1]. Figure 4a presents 23 genes with half-lives of less than 4 hours for which the average expression in six cell lines was fourfold greater than the average expression in three CLL samples. This selection criteria identified c-*myc*, a gene previously known to have a short-lived mRNA, and an obviously important target of flavopiridol given its role in G1/S phase progression [26]. Interestingly, roughly half of these genes (11/23) are expressed preferentially in M phase and/or encode proteins involved in M-phase events. These genes represent important targets of flavopiridol action as they encode M-phase regulatory kinases (PLK, aurora/IPL1-related kinase, and ckshs2), M-phase checkpoint proteins (CHK1), and chromosome segregation proteins (CENP-E, CENP-F) (Figure 4a). Given the relatively short duration of M phase in most cells, the short half-lives of these mRNAs may be important to ensure that key M-phase regulators are not expressed as the cell progresses from M to G1 phase.

Another important class of genes that might contribute to the efficacy of flavopiridol would include anti-apoptotic genes with rapid mRNA turnover (Figure 4b). Two anti-apoptotic Bcl-2 family members that were expressed in OCI-Ly3 cells - A1 and MCL1 - had mRNA half-lives shorter than 3 hours. Three members of the IAP family (c-IAP1, c-IAP2, NAIP) had very short mRNA half-lives and encode anti-apoptotic proteins that act by directly binding to caspases 3, 7, and 9 [27]. The NF-κB target gene *A20*, an inhibitor of tumor necrosis factor (TNF)-induced apoptosis [28], is expressed in OCI-Ly3 cells and had a very short mRNA half-life. As TNF-α is expressed by OCI-Ly3 cells, inhibition of A20 expression by flavopiridol treatment may contribute to its cytotoxic effect on these cells. In accord with these results, flavopiridol treatment was recently shown to down-regulate two of these anti-apoptotic proteins, MCL1 and Bag-1, and induce apoptosis in B-CLL cells treated with flavopiridol [29].

The majority of the genes with labile mRNAs, however, did not fall into the cell cycle or apoptosis categories but instead included many genes that are known to be inducible by cellular signaling. For example, transcription factors belonging to the NF-κB family are activated by a wide variety of cellular signaling events, and several known NF-κB target genes (*A1, A20*, c-IAP1, c-IAP2, IκB alpha, IκB epsilon, CD54, IL-6, IL-8, TNF-α, IRF-4*) were found to have unstable mRNAs (Figure 4d). This observation led us to investigate the possibility that the class of genes that are transcriptionally induced by cellular signaling events is enriched for genes with labile mRNAs. We used Lymphochip microarrays to

Figure 4
Analysis of genes inhibited by flavopiridol. OCI-Ly3 cells were treated with flavopiridol (1 μM) for 0.5, 2, 3, 4, 6 or 8 h. Total RNA was prepared for microarray analysis on Lymphochips with approximately 17,000 microarray elements. The treated samples were labeled red (Cy5) and untreated samples were labeled green (Cy3). Genes were first categorized according to their half-lives using the scheme as described in the Materials and methods section. These genes were then clustered according to their function. **(a)** Proliferation genes with half-lives of less than 4 h. The cell-cycle phase in which the particular gene is expressed is indicated. **(b)** Anti-apoptotic genes with short half-lives. **(c)** Percentages of induced or not-induced microarray elements as categorized by their half-lives. **(d)** Induced genes with half-lives of less than 4 h. See text for details.

profile the changes in gene expression that occurred in response to a wide variety of signaling events: B-cell lymphoma cell lines stimulated by crosslinking the B-cell antigen receptor or by treatment with phorbol ester and ionomycin (PI), resting peripheral blood T cells stimulated with PI, and peripheral blood monocytes stimulated with lipopolysaccharide. Figure 4d shows genes with relatively short mRNA half-lives (< 2 hours and 2-4 hours) that were also transcriptionally induced at least threefold in one of the cellular activation experiments described above. Roughly one third of the inducible genes in OCI-Ly3 cells were in this rapid mRNA turnover category (Figure 4c). By contrast, 16.8% of the genes that were not induced by these stimuli had mRNA half-lives of less than 4 hours ($P < 0.001$).

This analysis of mRNA turnover in OCI-Ly3 cells therefore suggested that transcriptionally inducible genes are, as a class, likely to generate labile mRNAs. To test this notion, we profiled mRNA turnover rates in peripheral blood mononuclear cells (PBMCs) after stimulation with PI. PBMCs were stimulated with PI for 3 hours, at which time flavopiridol was added and mRNA levels were subsequently determined by microarray analysis. Genes were assigned to the inducible class if their mRNA levels increased more that fourfold by PI in 3 hours. As shown in Figure 5a, a substantial proportion (44%) of the inducible genes had mRNA half-lives shorter than 2 hours. By contrast, only 11% of the non-inducible class of genes had mRNA half-lives less than 2 hours, and more than 70% of these genes had mRNA half-

lives longer than 6 hours ($P < 0.001$) (Figure 5a). This result confirmed, in an independent cellular system, the observation that transcriptionally inducible genes preferentially encode rapidly degraded mRNAs.

We next investigated the functional characteristics of the genes assigned to each mRNA turnover class (Figure 5b). More than one third of genes regulating apoptosis were both inducible and had mRNA half-lives of less than 2 hours. By contrast, only 10% of the genes encoding cell-surface proteins were in this class. The apoptosis regulators included several anti-apoptotic genes discussed previously (*A20, MCL1,* c-*IAP2*), as well as potentially pro-apoptotic genes such as those for Fas ligand and TNF receptor type II. PHLDA1 is the human homolog of TDAG51, a pleckstrin-homology domain protein that may modulate apoptosis by regulating Fas ligand expression following stimulation through the T-cell receptor. It is well known that apoptosis in T lymphocytes is an elaborately orchestrated process following lymphocyte activation that allows clonal expansion of the activated T cells while eventually eliminating the clone through the process of activation-induced cell death [30]. Thus, anti-apoptotic gene products are required early during lymphocyte activation, whereas attenuation of the clonal burst eventually requires pro-apoptotic signaling through Fas and the TNF receptors. This change in apoptotic responsiveness may be accomplished rapidly by combining transcriptional regulation with rapid mRNA turnover of key apoptosis regulatory genes.

Transcriptional reprogramming following lymphocyte activation involves the coordinate induction of transcription factors [31] and many of these were found to have labile mRNAs (Figure 5b). Several of these genes are known to encode immediate early transcription factors (for example, FosB, NAB2, ATF-3, NOT1) that are induced by a wide range of cellular stimuli, and this class of transcription factors is well known to have unstable mRNAs [32]. Other inducible transcription factors with labile mRNAs have more lymphocyte-specific functions such as IRF-4, a factor that is required for lymphocyte activation but is not required in other lineages [33].

Not surprisingly, the most inducible class of genes in PBMCs encoded cytokines, chemokines and their receptors (Figure 5c). Within this class, more than 25% of genes had mRNA half-lives of less than 2 hours. As expected, many cytokine mRNAs were both rapidly inducible and rapidly degraded (Figure 5d). Unexpectedly, the chemokine genes had much more stable mRNAs than the cytokine genes, even though they were strongly induced by PI treatment (Figure 5d). The mRNAs for the cytokine and chemokines receptors also differed in their stability. The inducible chemokine receptors CCR1 and CXCR5 had labile mRNAs, whereas most of the inducible cytokine receptors (IL-2, IL-3, IL-6 receptor α chains) had relatively stable mRNAs. The

differential mRNA stabilities of cytokines, chemokines and their receptors reflect their divergent biological functions. Cytokines potently induce activation and differentiation of target cells in a tightly regulated temporal fashion during immune responses [34]. To limit inappropriate effects of cytokines both temporally and spatially on bystander cells, the levels of these factors must be modulated rapidly, which can be achieved given their short mRNA half-lives. On the other hand, chemokines are chemoattractants that signal leukocyte migration by setting up concentration gradients that are recognized by chemokine receptors [35]. The inducible chemokines are used in inflammatory responses and wound healing to attract the appropriate complement of immune cells to the affected tissues. These cellular reactions need to be rapidly initiated but are slowly resolved, a kinetic profile that can be understood in light of the relative stability of chemokine mRNAs.

Finally, we investigated whether known *cis*-acting mRNA motifs could account for the mRNA turnover rates measured in the present study. Adenylate-uridylate-rich elements (AREs) mediate rapid turnover of some mRNAs. Three different classes of ARE have been defined, two of which include the core motif AUUUA [13]. A recent bioinformatics analysis of labile mRNAs with AUUUA motifs extended this core motif to the nonamer UAUUUAWW, and a database of mRNAs that have matches to this motif in their 3′ untranslated regions was created [36]. Using this database, we examined the distribution of these AU-rich motifs among the classes of mRNAs with different half-lives. Figure 6 shows that this motif was found preferentially in the most unstable mRNAs and was observed with decreasing frequency in mRNAs with longer half-lives. Nonetheless, 10% of the genes in the long half-life category (> 8 hours) contained AREs, demonstrating that the ARE motif is not completely predictive of rapid mRNA turnover. Furthermore, many of the RNAs with unstable mRNAs lacked the ARE consensus motif, suggesting that other *cis*-elements may be responsible for their rapid degradation.

Conclusions

The systematic determination of mRNA degradation rates described in the present report revealed an underlying logic that relates gene function and mRNA stability. The largest category of genes found to have unstable mRNAs included genes that were inducible by various cellular signaling events. The inducibility of many of these genes is known to be due to transcriptional activation of their promoters. Thus, the rapid degradation of these mRNAs allows their levels to rapidly drop when transcriptional activation is terminated. By categorizing genes using the functional properties of their encoded proteins, we found that certain functional classes were relatively enriched for unstable mRNAs. Two such classes, the cytokine genes and immediate early transcription factor genes, were previously known to have unstable
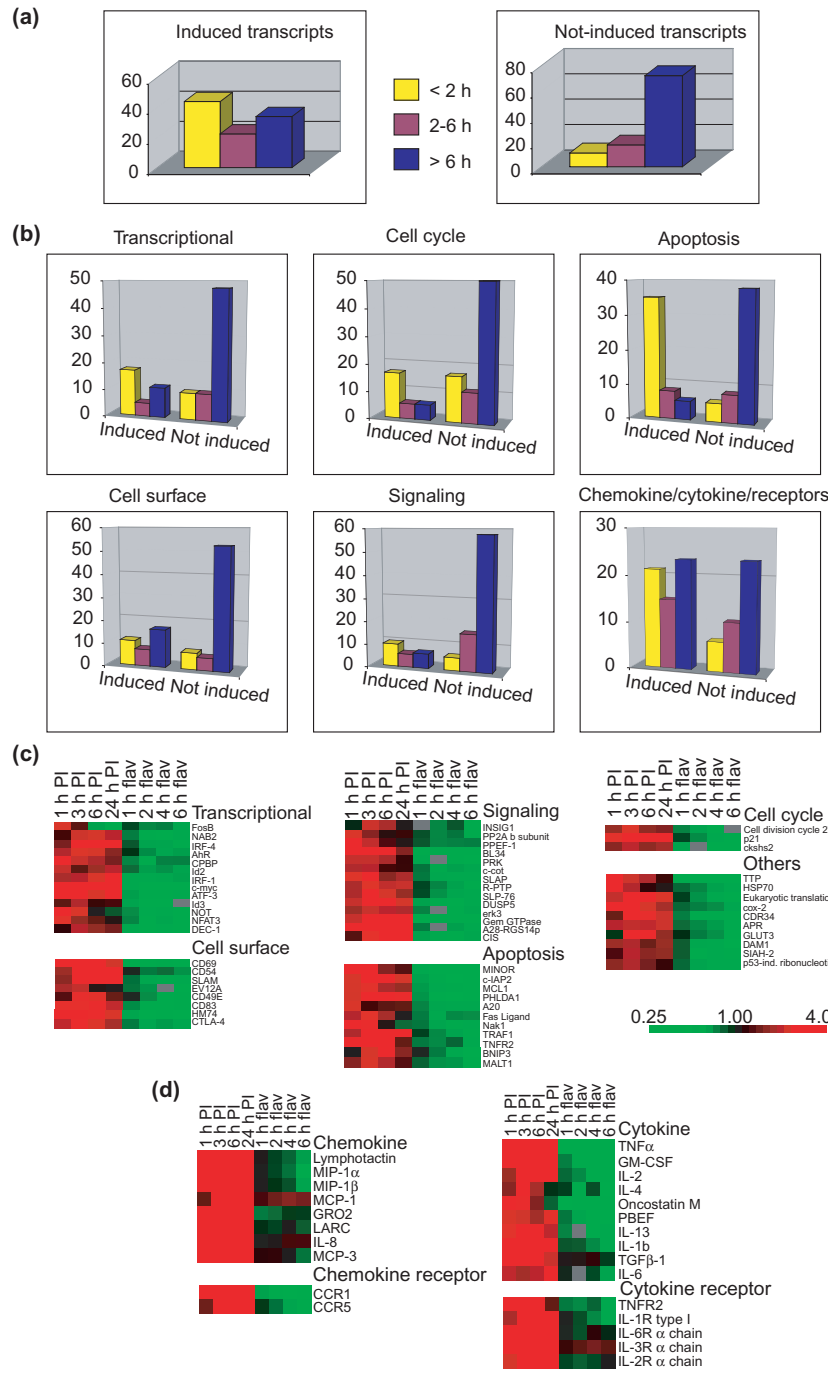
Figure 5
Subgrouping of induced genes of PBMCs. Purified PBMCs were induced with PI for 1, 3, 6 or 24 h before harvesting for microarray analysis. The induced samples were labeled red (Cy5) and uninduced samples were labeled green (Cy3). For analyzing the turnover rate of these induced transcripts, purified PBMCs were first induced with PI treatment for 3 h followed by flavopiridol treatment for 1, 2, 4 or 6 h before harvesting for microarray analysis. The induced samples treated with flavopiridol were labeled red (Cy5) and induced samples without flavopiridol treatment were labeled green (Cy3). **(a)** Percentages of genes (induced or not induced by PI) are plotted according to their half-lives (indicated by the different colors). **(b)** Percentages of genes of certain functional groups (induced or not induced by PI) are plotted according to their half-lives. **(c)** Microarray data showing highly induced genes with short half-lives of certain functional groups. **(d)** Microarray data showing half-lives of highly induced chemokines, cytokines and their receptors.
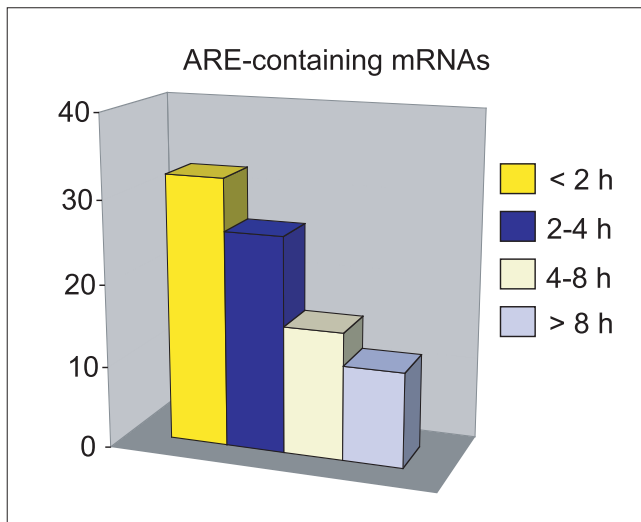
Figure 6
Percentages of AUUUA-containing transcripts in different half-life groups.

mRNAs. The class of apoptosis regulators, however, was not previously known to be enriched for labile mRNAs. However, given the need to rapidly modulate apoptosis during development, cellular differentiation, and immune responses, this property of the apoptotic genes can be readily understood. Another unanticipated finding was that many critical regulators of M phase of the cell cycle had rapidly degraded mRNAs. In light of the short duration of M phase, these labile M-phase regulators may need to be eliminated rapidly to allow correct entry into G1 phase of the cell cycle.

The initial impetus of this research was to understand the mechanism of action of the anti-cancer drug flavopiridol. The regulatory logic of mRNA degradation revealed in this study gives us insight into how this general transcriptional inhibitor can have selective toxicity for tumor cells. In particular, the short half-lives of mRNAs encoding M-phase proteins and other key cell-cycle regulators (for example, c-Myc) may contribute to the cytotoxicity of flavopiridol for cancer cells but may also contribute to the dose-limiting toxicity of flavopiridol for gut epithelium, leading to secretory diarrhea [16]. However, the present results also suggest that flavopiridol may be more effective in treating certain types of cancer cells that are highly dependent on genes with unstable mRNAs. For example, OCI-Ly3 lymphoma cells constitutively express two anti-apoptotic BCL-2 family members, A1 and MCL1, which are not expressed at high levels in normal lymphocytes. The instability of the A1 and MCL1 mRNAs therefore may contribute to the toxicity of flavopiridol for these lymphoma cells. Gene expression profiling demonstrated that the OCI-Ly3 cell line is an excellent model for the activated B-like DLBCL subtype [1]. Indeed, fresh lymphoma biopsies from such patients revealed high expression

of A1 and MCL1 in most cases [1]. These results suggest that activated B-like DLBCL might be a particularly attractive candidate disease for new clinical trials of flavopiridol.

Materials and methods
Chemicals and cells
Flavopiridol and 9-nitropaullone were obtained from the NCI Developmental Therapeutics Program. DRB, MTT (3-(4,5-dimethylthiazol-2-yl)-2,5-diphenyltetrazolium bromide) and ionomycin were purchased from Sigma. Actinomycin D, roscovitine, phorbol ester and lipopolysaccharide (LPS) were purchased from Calbiochem. Anti-human IgM was purchased from Jackson ImmunoResearch Laboratories, Inc.

Primary T cells and monocytes were purified from human blood by magnetic cell sorting. PBMCs were purified by Ficoll density gradient centrifugation. OCI-Ly1 and OCI-Ly3 were maintained in Iscove's modified essential medium with β-mercaptoethanol (55 μM), penicillin (50 units/ml), streptomycin (50 μg/ml), and 20% heparinized normal human plasma. SUDHL-5, SUDHL-6, WSU-1, Jurkat, MCF-7, PC3, BJAB, T cells, monocytes and PBMCs were maintained in RPMI 1640 medium with L-glutamine, HEPES, penicillin, streptomycin and 10% fetal bovine serum. Cells were grown in a 37°C incubator in the presence of 5% carbon dioxide. PBMCs (except the activation time course) and T cells were stimulated for 3 h with phorbol ester (50 ng/ml) and ionomycin (1.5 μM). B cell lines were stimulated with anti-IgM antibody (50 μg/ml). Monocytes were stimulated for 3 h with LPS (0.2 μg/ml). CLL samples and cell lines used for clustering in Figure 4a were prepared according to Alizadeh et al. [1]. For all experiments, 1 μM flavopiridol was used (except the titration experiment in Figure 1a). PBMCs were first activated at 5×10^6 cells/ml with PI for 3 h before flavopiridol treatment. The activation of the PBMCs by PI treatment was confirmed by FACS analysis of CD69 and CD44 expression.

MTT assays
MTT assays were done as described [37]. In brief, OCI-Ly3 cells grown in 96-well plates were treated with increasing concentration of flavopiridol (0 to 2 μM) for 8, 24 or 48 h. MTT was added to the cells 2 h before harvesting. Cells were lysed completely in isopropanol with 1% hydrochloric acid. The plate was read with a 96-well spectrometer using a 570-nm filter. The background was subtracted using a dual-wavelength setting of 570 and 630 nm.

Microarray analysis and northern blotting
Microarray analysis was performed as described [38]. Total RNA was prepared using Trizol reagent (Gibco BRL) according to the manufacturer's instruction. For each sample, 40 μg of total RNA was used for the labeling reaction. All primary microarray data are available at our website [39].

Ten micrograms of total RNA were used for northern blot analysis. The probes were prepared from PCR amplification of the cDNA clones used for printing the Lymphochip.

Data analysis

The raw data from each cDNA array were normalized as described [38]. Data extracted must fulfill the following criteria. Spot size must be > 25 μm and expression levels for all flavopiridol studies must be > 500 relative fluorescent units (RFU) for the Cy3 channel, and > 0 RFU for the Cy5 channel; PBMC induction studies: > 50 RFU for both channels.

For the half-life studies in Figures 2,4,5, the array elements (genes) were selected for each of the indicated time points (Figure 7, X h for example) on the basis of three criteria. First, the mRNA abundance at X h, as measured by the ratio of the array element (Cy5/Cy3) must have decreased by at least twofold. Second, the average of the geometric means for the array element at the later time points (for example, Z1, Z2, and Z3) must be less than the twofold decrease of that element at the indicated time point. Third, the average of the geometric means for previous time points (for example, Y1 and Y2) must be greater than the twofold decrease of that element at the indicated time point.

The expression data for array elements representing the same gene were averaged. Hierarchical clustering was performed using Cluster software and visualized using the Tree View software [40].

ARE-mRNA database

The accession numbers of transcripts with one to five copies of AUUUA were downloaded from the ARE-mRNA database [41]. These transcripts were categorized by their half-lives according to the PBMC database.

Mathematical analysis of mRNA half-lives

A first-order kinetic model would imply that the log-ratio of Cy5 to Cy3 would decrease linearly with time. For each gene,
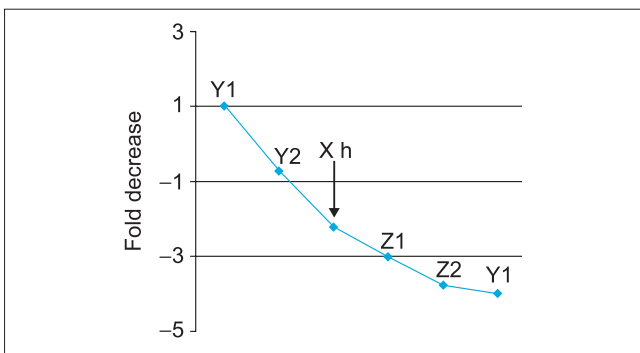
we fitted a linear regression model of the log-ratios to the time points, where the model included a separate intercept and coefficient term for each of the three drugs:

$$\log_2(Cy5/Cy3) = (\alpha_{Flav} + \beta_{Flav}\, t) * I_{[Flav]} + (\alpha_{ActD} + \beta_{ActD}\, t) * I_{[ActD]} + (\alpha_{DRB} + \beta_{DRB}\, t) * I_{[DRB]}\,,$$

where t denotes the time in hours; $I_{[.]}$ denotes an indicator function for the treatment drug, taking the values 0 or 1, depending on whether or not that treatment drug was used for the Cy5 measurement of that log-ratio; and α_{Flav}, β_{Flav}, α_{ActD}, β_{ActD}, α_{DRB}, and β_{DRB} are model parameters to be estimated.

Although each drug was allowed to have a distinct first-order degradation rate in the model, the three drugs were assumed to have identical error distributions in their assay variability. The mRNA half-life for each drug treatment was computed as the negative of the inverse of the coefficient for each drug:

$$t_{Flav} = -1/\beta_{Flav}\,, \quad t_{ActD} = -1/\beta_{ActD}\,, \quad t_{DRB} = -1/\beta_{DRB}.$$

Statistical analysis

The following test [42], was used to evaluate whether the proportion of induced genes with half-life less than 2 h is statistically different from the proportion of not induced genes with half-life less than 2 h, for both the OCI-Ly3 (Figure 4c) and PBMC (Figure 5a):

$$z = (\,|\,p_2 - p_1\,| - 1/2 * (1/n_1 + 1/n_2)\,) / (p * q * (1/n_1 + 1/n_2)\,)^{1/2}\,,$$

where n_1 = number of the induced genes, n_2 = number of the not induced genes, p_1 = proportion of induced genes with half-life less than 2 h, p_2 = proportion of not-induced genes with half-life less than 2 h, p = overall proportion of genes with half-life less than 2 hours, and $q = 1 - p$.

Additional data files

The following additional data files containing the primary data for the figures are included with the online version of this article: Figure 1a, flavopiridol titration; Figure 1c, Cdk inhibitors; Figure 2a, flavopiridol, actinomycin D and DRB; Figure 3, half-lives of well-measured genes; Figure 4a, proliferation genes; Figure 4b, anti-apoptotic genes; Figure 4d, induced genes in OCI -Ly3 cells; Figure 5c, highly induced genes in PBMC; Figure 5d, highly induced chemokines, cytokines and their receptors.

Figure 7
Scheme for determining half-lives in Figures 2, 4 and 5. See Materials and methods for details.

References
1.	Alizadeh AA, Eisen MB, Davis RE, Ma C, Lossos IS, Rosenwald A, Boldrick JC, Sabet H, Tran T, Yu X, *et al.*: **Distinct types of diffuse**

large B-cell lymphoma identified by gene expression profiling. *Nature* 2000, **403:**503-511.

2. Bittner M, Meltzer P, Chen Y, Jiang Y, Seftor E, Hendrix M, Radmacher M, Simon R, Yakhini Z, Ben-Dor A, *et al.*: **Molecular classification of cutaneous malignant melanoma by gene expression profiling.** *Nature* 2000, **406:**536-540.

3. Perou CM, Sorlie T, Eisen MB, van de Rijn M, Jeffrey SS, Rees CA, Pollack JR, Ross DT, Johnsen H, Akslen LA, *et al.*: **Molecular portraits of human breast tumours.** *Nature* 2000, **406:**747-752.

4. Carlson B, Pearlstein R, Naik R, Sedlacek H, Sausville E, Worland P: **Inhibition of CDK2, CDK4 and CDK7 by flavopiridol and structural analogs.** *Proc Am Assoc Cancer Res* 1996, **37:**424.

5. De Azevedo WF Jr, Mueller-Dieckmann HJ, Schulze-Gahmen U, Worland PJ, Sausville E, Kim SH: **Structural basis for specificity and potency of a flavonoid inhibitor of human CDK2, a cell cycle kinase.** *Proc Natl Acad Sci USA* 1996, **93:**2735-2740.

6. Gray NS, Wodicka L, Thunnissen AM, Norman TC, Kwon S, Espinoza FH, Morgan DO, Barnes G, LeClerc S, Meijer L, *et al.*: **Exploiting chemical libraries, structure, and genomics in the search for kinase inhibitors.** *Science* 1998, **281:**533-538.

7. Senderowicz AM, Sausville EA: **Preclinical and clinical development of cyclin-dependent kinase modulators.** *J Natl Cancer Inst* 2000, **92:**376-387.

8. Worland PJ, Kaur G, Stetler-Stevenson M, Sebers S, Sartor O, Sausville EA: **Alteration of the phosphorylation state of p34cdc2 kinase by the flavone L86-8275 in breast carcinoma cells. Correlation with decreased H1 kinase activity.** *Biochem Pharmacol* 1993, **46:**1831-1840.

9. Senderowicz AM: **Flavopiridol: the first cyclin-dependent kinase inhibitor in human clinical trials.** *Invest New Drugs* 1999, **17:**313-320.

10. Parker BW, Kaur G, Nieves-Neira W, Taimi M, Kohlhagen G, Shimizu T, Losiewicz MD, Pommier Y, Sausville EA, Senderowicz AM: **Early induction of apoptosis in hematopoietic cell lines after exposure to flavopiridol.** *Blood* 1998, **91:**458-465.

11. Chao SH, Fujinaga K, Marion JE, Taube R, Sausville EA, Senderowicz AM, Peterlin BM, Price DH: **Flavopiridol inhibits P-TEFb and blocks HIV-1 replication.** *J Biol Chem* 2000, **275:**28345-28348.

12. Price DH: **P-TEFb, a cyclin-dependent kinase controlling elongation by RNA polymerase II.** *Mol Cell Biol* 2000, **20:**2629-2634.

13. Chen CY, Shyu AB: **AU-rich elements: characterization and importance in mRNA degradation.** *Trends Biochem Sci* 1995, **20:**465-470.

14. Brown CY, Lagnado CA, Goodall GJ: **A cytokine mRNA-destabilizing element that is structurally and functionally distinct from A+U-rich elements.** *Proc Natl Acad Sci USA* 1996, **93:**13721-13725.

15. Alizadeh A, Eisen M, Davis RE, Ma C, Sabet H, Tran T, Powell JI, Yang L, Marti GE, Moore DT, *et al.*: **The lymphochip: a specialized cDNA microarray for the genomic-scale analysis of gene expression in normal and malignant lymphocytes.** *Cold Spring Harb Symp Quant Biol* 1999, **64:**71-78.

16. Senderowicz AM, Headlee D, Stinson SF, Lush RM, Kalil N, Villalba L, Hill K, Steinberg SM, Figg WD, Tompkins A, *et al.*: **Phase I trial of continuous infusion flavopiridol, a novel cyclin-dependent kinase inhibitor, in patients with refractory neoplasms.** *J Clin Oncol* 1998, **16:**2986-2999.

17. Gray N, Detivaud L, Doerig C, Meijer L: **ATP-site directed inhibitors of cyclin-dependent kinases.** *Curr Med Chem* 1999, **6:**859-875.

18. Alessi F, Quarta S, Savio M, Riva F, Rossi L, Stivala LA, Scovassi AI, Meijer L, Prosperi E: **The cyclin-dependent kinase inhibitors olomoucine and roscovitine arrest human fibroblasts in G1 phase by specific inhibition of CDK2 kinase activity.** *Exp Cell Res* 1998, **245:**8-18.

19. Meijer L, Borgne A, Mulner O, Chong JP, Blow JJ, Inagaki N, Inagaki M, Delcros JG, Moulinoux JP: **Biochemical and cellular effects of roscovitine, a potent and selective inhibitor of the cyclin-dependent kinases cdc2, cdk2 and cdk5.** *Eur J Biochem* 1997, **243:**527-536.

20. Pippin JW, Qu Q, Meijer L, Shankland SJ: **Direct *in vivo* inhibition of the nuclear cell cycle cascade in experimental mesangial proliferative glomerulonephritis with Roscovitine, a novel cyclin-dependent kinase antagonist.** *J Clin Invest* 1997, **100:**2512-2520.

21. Planchais S, Glab N, Trehin C, Perennes C, Bureau JM, Meijer L, Bergounioux C: **Roscovitine, a novel cyclin-dependent kinase inhibitor, characterizes restriction point and G2/M transition in tobacco BY-2 cell suspension.** *Plant J* 1997, **12:**191-202.

22. Gussio R, Zaharevitz DW, McGrath CF, Pattabiraman N, Kellogg GE, Schultz C, Link A, Kunick C, Leost M, Meijer L, Sausville EA: **Structure-based design modifications of the paullone molecular scaffold for cyclin-dependent kinase inhibition.** *Anticancer Drug Des* 2000, **15:**53-66.

23. Schultz C, Link A, Leost M, Zaharevitz DW, Gussio R, Sausville EA, Meijer L, Kunick C: **Paullones, a series of cyclin-dependent kinase inhibitors: synthesis, evaluation of CDK1/cyclin B inhibition, and *in vitro* antitumor activity.** *J Med Chem* 1999, **42:**2909-2919.

24. Zaharevitz DW, Gussio R, Leost M, Senderowicz AM, Lahusen T, Kunick C, Meijer L, Sausville EA: **Discovery and initial characterization of the paullones, a novel class of small-molecule inhibitors of cyclin-dependent kinases.** *Cancer Res* 1999, **59:**2566-2569.

25. Perou CM, Jeffrey SS, van de Rijn M, Rees CA, Eisen MB, Ross DT, Pergamenschikov A, Williams CF, Zhu SX, Lee JC, *et al.*: **Distinctive gene expression patterns in human mammary epithelial cells and breast cancers.** *Proc Natl Acad Sci USA* 1999, **96:**9212-9217.

26. Dang CV: **c-Myc target genes involved in cell growth, apoptosis, and metabolism.** *Mol Cell Biol* 1999, **19:**1-11.

27. Deveraux QL, Reed JC: **IAP family proteins - suppressors of apoptosis.** *Genes Dev* 1999, **13:**239-252.

28. Lee EG, Boone DL, Chai S, Libby SL, Chien M, Lodolce JP, Ma A: **Failure to regulate TNF-induced NF-kappaB and cell death responses in A20-deficient mice.** *Science* 2000, **289:**2350-2354.

29. Kitada S, Zapata JM, Andreeff M, Reed JC: **Protein kinase inhibitors flavopiridol and 7-hydroxy-staurosporine down-regulate antiapoptosis proteins in B-cell chronic lymphocytic leukemia.** *Blood* 2000, **96:**393-397.

30. Lenardo M, Chan KM, Hornung F, McFarland H, Siegel R, Wang J, Zheng L: **Mature T lymphocyte apoptosis - immune regulation in a dynamic and unpredictable antigenic environment.** *Annu Rev Immunol* 1999, **17:**221-253.

31. Kuo CT, Leiden JM: **Transcriptional regulation of T lymphocyte development and function.** *Annu Rev Immunol* 1999, **17:**149-187.

32. Chen CY, Shyu AB: **Selective degradation of early-response-gene mRNAs: functional analyses of sequence features of the AU-rich elements.** *Mol Cell Biol* 1994, **14:**8471-8482.

33. Mittrucker HW, Matsuyama T, Grossman A, Kundig TM, Potter J, Shahinian A, Wakeham A, Patterson B, Ohashi PS, Mak TW: **Requirement for the transcription factor LSIRF/IRF4 for mature B and T lymphocyte function.** *Science* 1997, **275:**540-543.

34. Balkwill F: In *The Cytokine Network.* Edited by Balkwill F. Oxford: Oxford University Press, 2000.

35. Sallusto F, Mackay CR, Lanzavecchia A: **The role of chemokine receptors in primary, effector, and memory immune responses.** *Annu Rev Immunol* 2000, **18:**593-620.

36. Bakheet T, Frevel M, Williams BR, Greer W, Khabar KS: **ARED: human AU-rich element-containing mRNA database reveals an unexpectedly diverse functional repertoire of encoded proteins.** *Nucleic Acids Res* 2001, **29:**246-254.

37. Davis LS, Lipsky PE, Bottomly K: In *Current Protocols in Immunology.* Edited by Coligan JE, Kruisbeek AM, Margulies DH, Shevach EM, Strober W. New York: John Wiley & Sons, 1994.

38. Shaffer AL, Yu X, He Y, Boldrick J, Chan EP, Staudt LM: **BCL-6 represses genes that function in lymphocyte differentiation, inflammation, and cell cycle control.** *Immunity* 2000, **13:**199-212.

39. **Staudt Laboratory (mRNA turnover studies using DNA microarrays)**
[http://lymphochip.nih.gov/mRNAturnover/LLweb/Homepage.html]

40. Eisen MB, Spellman PT, Brown PO, Botstein D: **Cluster analysis and display of genome-wide expression patterns.** *Proc Natl Acad Sci USA* 1998, **95:**14863-14868.

41. **ARE-mRNA database (ARED)** [http://rc.kfshrc.edu.sa/ared]

42. Fleiss, JH: In *Statistical Methods for Rates and Proportions.* New York: John Wiley & Sons, 1981.